Defocused point spread function of asymmetrically apodized optical imaging systems with slit apertures

Andra Naresh Kumar Reddy[1,2*], and Dasari Karuna Sagar[3]

[1] Science and Research Laboratory of Automated Systems of Science Researches, Samara National Research University, 34 Moskovskoye Shosse, Samara, 443086, Russia

[2] Department of Physics (H&S), CMR Institute of Technology, Kandlakoya, Medchal Road, Hyderabad 501 401, Telangana, India

[3] Department of Physics, University College of Science, Osmania University Hyderabad-500007, India

[*] **e-mail:** naarereddy@gmail.com

Abstract. In the presence of defocusing, the PSF of an optical imaging system with asymmetric apodization have been investigated analytically. The asymmetry in the PSF has been observed to increase with edge strip width (b) of the slit aperture and further improved by defect of focus in the image plane, permits to achieve a significant improvement in side-lobe suppression. The proposed analytical model of pupil function considers these effects and formulates a space-variant PSF is obtained by employing asymmetric apodization. The optimum values for asymmetric apodization controlling parameter (b) and defocusing parameter (Y) at which results in smoothing the central peak shape and reducing optical side-lobes intensity on one side of the Asymmetric PSF termed as 'good' side at the cost of worsening its counterpart known as 'bad side' with which renders the resolution of apodized optical imaging systems. In order to simplify the proposed analytical design an efficient method is derived and evaluated. © 2016 Journal of Biomedical Photonics & Engineering.

Keywords: defocusing, diffraction, asymmetric apodization, two-line resolution, point spread function, complex pupil function.

Paper #3046 received 2016.05.28; revised manuscript received 2016.09.05; accepted for publication 2016.09.29; published online 2016.09.30. doi: 10.18287/JBPE16.02.030302

References

1. H. H. Hopkins, "The Frequency Response of a Defocused Optical System," Proceedings of the Royal Society A: Mathematical, Physical and Engineering Sciences 231(1184), 91–103 (1955).
2. P. A. Stokseth, "Properties of a Defocused Optical System," J. Opt. Soc. Am. 59(10), 1314 (1969).
3. J. Li, P. Agathoklis, F. Peet, G. Jensen, and T. Sahota, "Measurement and analysis of defocused point spread functions and optical transfer functions of a microscope," IEEE Pacific Rim Conference on Communications, Computers, and Signal Processing (1995).
4. A. R. FitzGerrell, E. R. Dowski, and W. T. Cathey, "Defocus transfer function for circularly symmetric pupils," Applied Optics 36(23), 5796 (1997).
5. I. Klapp, and Y. Yitzhaky, "Angular motion point spread function model considering aberrations and defocus effects," J. Opt. Soc. Am. A 23(8), 1856 (2006).
6. J. Burge, and W. S. Geisler, "Optimal Image-based Defocus Estimates from Individual Natural Images," Imaging and Applied Optics (2011).
7. X. Zhu, S. Cohen, S. Schiller, and P. Milanfar, "Estimating Spatially Varying Defocus Blur From A Single Image," IEEE Transactions on Image Processing 22(12), 4879–4891 (2013).
8. A. Greengard, Y. Y. Schechner, and R. Piestun, "Depth from diffracted rotation," Opt. Lett. 31(2), 181 (2006).
9. P. Favaro, and S. Soatto, "A geometric approach to shape from defocus," IEEE Transactions on Pattern Analysis and Machine Intelligence 27(3), 406–417 (2005).
10. C.-Y. Wen, and C.-H. Lee, "Point spread functions and their applications to forensic image restoration Introduction," Forensic Science Journal 1(1), 15-26 (2002).

11. G. O. Reynolds, J. B. Deveils, J. B. Parrent Jr, and B. J. Thompson, "The New Physical optic notebook: Tutorials in Fourier Optics," SPIE Optical Engineering Press, Bellingham, WA and New York (1989).
12. D. N. Grimes, and B. J. Thompson, "Two-Point Resolution with Partially Coherent Light," J. Opt. Soc. Am. 57(11), 1330 (1967).
13. F. Rojak, MS Thesis, Lowell Technological Institute, Lowell, MA (1961).
14. B. J. Beran, and J. B. Parrent Jr, The theory of partial coherence, Pentice Hall Englewood Cliff, NJ, 124 (1964).
15. O. Falconi, "Limits to which Double Lines, Double Stars, and Disks can be Resolved and Measured," J. Opt. Soc. Am. 57(8), 987 (1967).
16. F. Kottler, and F. H. Perrin, "Imagery of One-Dimensional Patterns," J. Opt. Soc. Am. 56(3), 377 (1966).
17. S. V. Gupta, and D. Sen, "Diffrimoscopic image formation under partial coherent illumination (Slits and Opaque strips)," Optica Acta: J. Opt. 18(10), 779-792 (1971).
18. R. S. Sirohi, "Limit of resolution of diffraction limited circular aperture for line objects," Optik 29, 437-439 (1969).
19. D. Karuna Sagar, G. Bikshamaiah, and S. Lacha Goud, "Resolution of two-line objects by Hanning pupil functions of apodized optical systems under coherent illumination," Atti Fond. Giorgio Ronchi 61, 559 (2006).
20. P. K. Mondal, M. L. Calvo, and M. Chevaliar, "Resolution criterion and contrast factor for resolving two-line images under coherent and incoherent illumination," Proc. SPIE 1319, Optics in Complex Systems 378 (1990).
21. P. K. Mondal, M. L. Calvo, M. Chevaliar, and V. Lakshminarayanan, "Theoretical approach to hyperacuity tests based on resolution criteria for two-line images," Proc. SPIE 1429, Holography, Interferometry, and Optical Pattern Recognition in Biomedicine 108 (1991).
22. B. L. Metha, "Effect of non-uniform illumination on critical resolution by a circular aperture using partially coherent light," Atti Fond. Giorgio Ronchi 30, 17 (1975).
23. T. Asakura, "Resolution of two unequally bright points with partially coherent light," Nouvelle Revue d'Optique 5(3), 169–177 (1974).
24. H. H. Hopkins, and B. Zalar, "Aberration Tolerances Based on the Line Spread Function," Journal of Modern Optics 34(3), 371–406 (1987).
25. A. K. Pandey, G. S. Pant, and A. Malhotra, "Standardization of SPECT Filter Parameters," Indian Journal of Nuclear Medicine 19, 30-35 (2004).
26. L. Cheng, and G. G. Siu, "Asymmetric apodization," Measurement Science and Technology 2(3), 198–202 (1991).
27. G. G. Siu, L. Cheng, D. S. Chiu, and K. S. Chan, "Improved side-lobe suppression in asymmetric apodization," Journal of Physics D: Applied Physics 27(3), 459–463 (1994).
28. M. Keshavulu Goud, R. Komala, A. Naresh Kumar Reddy, and S. Goud, "Point Spread Function of Asymmetrically Apodized Optical Systems with Complex Pupil Filters: The One-Dimensional Case with Slit Aperture," Acta Physica Polonica A 122(1), 90–95 (2012).

1 Introduction

The Point Spread Function of image forming optical systems is determined by the parameters of the optical system and the distance or depth of the object being imaged. In real time imaging, defocused point spread functions are being used for the optical sectioning as part of microscope image visualization system. The response of a defocused optical system to line frequencies in the object studied analytically [1]. Pera A. Stokseth [2], has analyzed the optical properties of an aberration-free defocused optical system used to image incoherently illuminated objects. Li et al. [3] have measured and analyzed defocused point spread functions and optical transfer functions of a microscope. The main purpose of their analysis was to verify the accuracy of analytical approximations of these functions, which were presented but not extensively studied in the literature. Alan R. FitzGerrell et.al [4] presented a two-dimensional function that graphically illustrates the effects of defocus on the optical transfer function (OTF) associated with a circularly symmetric pupil function. All these studies were relative to defocusing analysis of Point Spread Function of optical systems with symmetric apodized pupils. I. Klapp and Y. Yitzhaky [5] developed new model of angular motion PSF by considering space -variant effects of wave front aberrations and defocus. J. Burge and W.S. Geisler [6] presented depth estimation algorithms for computational vision systems to estimate optimized defocus at each location in any individual natural image of human visual system. Xian Zhu et al. [7] proposed a method of algorithm for estimating spatially varying defocus in point spread function of an image, which is applicable to conventional optical imaging systems. Adam Greengard et al. [8] have shown the accuracy of depth estimation analytically based on defocus effects were improved significantly relative to classical methods by exploiting three-dimensional diffraction effects in optical microscopy. Paolo Favaro and Stefano Soatto [9] presented optimal technique to infer three-dimensional image shape from a collection of defocused images. Che–Yen Wen et al. [10] presented image

restoration techniques is to improve the visual quality of a degraded PSF of image due to motion turbulence, atmospheric turbulence. The theory of image formation considers the cases where the response to signals with complex geometrics is prerequisite along with the not completely characterized coherent function. One such example is the impulse response of an optical imaging system in the resolution of two line objects. The studies in this way are restricted to a few cases [11-25] principally concentrating the shaping and shading of the pupil function at focus. In this context, following Cheng and Siu [26] employed asymmetric apodization and succeeded in obtaining the so-called good side with very low side-lobes and sharp central peaks and the so-called bad side with enhanced side lobes and broader central peaks. It is obvious that the good side has been obtained at the cost of the bad side. In further continuation of their work [27] they obtained improved side-lobe suppression. Keshavulu et al. [28] investigated the Point spread function of asymmetrically apodized optical systems with one-dimensional case amplitude and phase filters. These studies are the basis for our investigation. We were further motivated by these studies [26-28], who initiated and developed the concept of asymmetric apodization, aimed at high resolution.

In the present study in addition to shading of complex pupil functions we investigate the performance of optical system in confocal imaging in terms of shift in pattern and side-lobe suppression for different out-of-focus planes. The effect of asymmetric apodization of slit functions is also studied for different out-of-focus planes i.e. collecting the PSFs of point object at different defocused image planes. Though we have reported the results but it extended to any other aperture of this nature in other regions of electromagnetic spectrum. The current study may also be considered in the field of visual optics for understanding of hyper–acuity tests based on the response of the human visual system to line pair stimulus. Importantly this study has significant importance to analyze the confocal imaging of line structures in close proximity.

2 Theory

Within the field of scalar diffraction optics, the amplitude impulse response of one-dimensional defocused optical imaging systems is the Fourier transform of the complex pupil function consists of three zones having uniform amplitude transmittance viz. two narrow strips at edges with opposite phase transmittances of the form exp (-$i\pi$/2) and exp ($i\pi$/2) and zero phase transmittance for the central cylindrical zone of the slit aperture. Because of exceptionally deep reduction ability and constant working angels throughout the regions of considered edge strips, we consider the antisymmetric phase functions. Thus we consider complex pupil function with real amplitude transmittance central zone and complex conjugated outer edge strips. In the presence of defocusing the resultant complex amplitude distribution $A(z)$ in the image plane is equal to the sum of the amplitude transmittance contributing by the central zone of the aperture, equals to unity and complex amplitudes contributing by the narrow left and right edge strips with opposite phase transmittances –i and i. The transmittance of the pupil function of the optical system is given by:

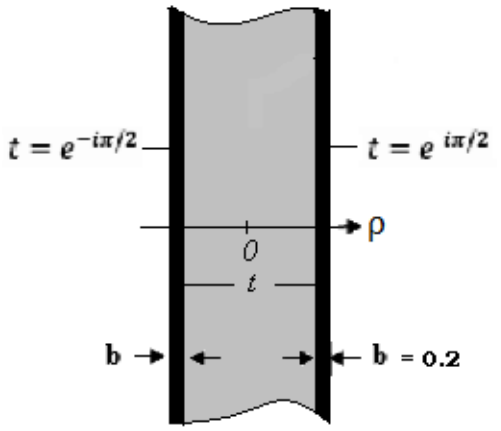

Fig. 1 Analytical design of one-dimensional asymmetric pupil function.

$$\begin{cases} \textit{Left edge strip} = -i, -1/2 \le \rho < -1/2 + b \\ \textit{Central zone} = 1, \quad -1/2 + b \le \rho \le 1/2 - b \\ \textit{Right edge strip} = +i, 1/2 - b < \rho \le 1/2 \end{cases} \tag{1}$$

The resultant diffraction field amplitude contributing by the three zones of the aperture is given by:

$$A(z) = \int_{-\frac{1}{2}}^{-\frac{1}{2}+b} -i\exp(i2z\rho)\,d\rho + \int_{-\frac{1}{2}+b}^{\frac{1}{2}-b} \exp\left[\frac{-iY\rho^2}{2}\right]\exp(i2z\rho)\,d\rho + \int_{\frac{1}{2}-b}^{\frac{1}{2}} i\exp(i2z\rho)\,d\rho, \tag{2}$$

where $z = k\sin\theta = \frac{2\pi}{\lambda}\sin\theta$, ρ is the coordinate in the pupil plane, z is the reduced dimensionless diffraction coordinate in the image plane, λ is the wavelength of the incident radiation and Y is the defocusing control parameter of the apodized optical imaging system.

The intensity of defocused PSF I(z) which is the real measurable quantity can be obtained by taking squared modulus of Eq.(2). Thus,

$$I(z) = |A(z)|^2. \tag{3}$$

3 Results and Discussion

The results of investigations on the asymmetric apodization effects on the defocusing diffracted PSF in the focal region of an optical imaging system have been obtained from Eq. (3) as function of diffraction

coordinate z varying from -10 to +10. An iterative twelve – point Gauss quadrature method of numerical integration has been developed and applied to obtain the positions and intensity of first dark ring and bright ring on either side of the diffraction center of the defocused PSF. Here we reported the positions and intensity values of central maxima, first minima and first maxima on good and bad sides of apodized PSF for defocused image planes. The range of values 'Y' takes from 0 to 2π in steps of π/2. These values have been evaluated for different values of edge strip width (b). Here [b = 0 and Y = 0] corresponds to Airy PSF.

Our study mainly concentrated on central peak shift, first minima positions (FMP) and first side lobe intensities (FSI) on good and bad side of the diffraction pattern since they are the important parameters in judging the resolution of defocused optical imaging systems with asymmetric apodization. It may be noticed that these values are computed for different cases and neglected higher order side-lobes and minima as they are suppressing fair enough to zero level. However, we reported the results for both good and bad sides which constitute the complete diffraction pattern of defocused optical imaging system.

Table 1 Intensities and positions of maxima and minima of the APSF for all values of b and Y.

b	Y	Central Maxima		FMP w.r.to z = 0		FMP w.r.to CMP	FSI	
		position	Intensity	good side	bad side	good side	good side	bad side
0	0	0	1	3.1416	-3.1416	3.1416	0.0471	0.0471
	π/2	0	0.9923	3.1513	-3.1513	3.1513	0.0461	0.0461
	π	0	0.9696	3.1809	-3.1809	3.1809	0.0429	0.0429
	3π/2	0	0.9328	3.2322	-3.2322	3.2322	0.0382	0.0382
	2π	0	0.8836	3.3084	-3.3084	3.3084	0.0323	0.0323
0.02	0	-0.132	0.9265	3.2828	-3.2647	3.4148	0.0285	0.0616
	π/2	-0.1329	0.9205	3.2928	-3.2721	3.4257	0.0278	0.0606
	π	-0.1358	0.9028	3.3234	-3.2949	3.4592	0.0258	0.0577
	3π/2	-0.1406	0.8739	3.3769	-3.3338	3.5175	0.0227	0.0531
	2π	-0.1479	0.835	3.457	-3.3903	3.6049	0.0189	0.0473
0.04	0	-0.2867	0.8669	3.4721	-3.3836	3.7588	0.0144	0.078
	π/2	-0.2883	0.8623	3.4833	-3.3893	3.7716	0.014	0.0771
	π	-0.2932	0.8487	3.5179	-3.4065	3.8111	0.0129	0.0744
	3π/2	-0.3016	0.8264	3.5787	-3.4358	3.8803	0.0112	0.0701
	2π	-0.3139	0.7962	3.6715	-3.4778	3.9854	0.0091	0.0644
0.06	0	-0.4584	0.8216	3.7711	-3.4999	4.2295	0.0056	0.0955
	π/2	-0.4604	0.8181	3.7862	-3.5042	4.2466	0.0054	0.0946
	π	-0.4663	0.8078	3.8332	-3.5172	4.2995	0.005	0.0921
	3π/2	-0.4763	0.791	3.9178	-3.539	4.3941	0.0045	0.0881
	2π	-0.4908	0.768	4.0512	-3.5701	4.542	0.0042	0.0828
0.08	0	-0.6377	0.7902	4.4815	-3.6152	5.1192	0.0072	0.113
	π/2	-0.6397	0.7876	4.5135	-3.6184	5.1532	0.0073	0.1122
	π	-0.6455	0.7799	4.6123	-3.6281	5.2578	0.0076	0.1099
	3π/2	-0.6555	0.7674	4.7813	-3.6443	5.4368	0.0083	0.1063
	2π	-0.6697	0.7502	5.007	-3.6672	5.6767	0.0093	0.1013
0.1	0	-0.8147	0.7713	5.6947	-3.7308	6.5094	0.0163	0.1292
	π/2	-0.8164	0.7694	5.7071	-3.7331	6.5235	0.0164	0.1285
	π	-0.8216	0.7638	5.7424	-3.7402	6.564	0.0169	0.1265
	3π/2	-0.8303	0.7545	5.7964	-3.7521	6.6267	0.0177	0.1233
	2π	-0.8426	0.7418	5.8631	-3.7689	6.7057	0.0188	0.1188

b	Y	Central Maxima		FMP w.r.to z = 0		FMP w.r.to CMP	FSI
		position	Intensity	good side	bad side	good side	good side	bad side
0.12	0	-0.9824	0.7629	6.1955	-3.8477	7.1779	0.0287	0.1428
	π/2	-0.9838	0.7616	6.2003	-3.8495	7.1841	0.0288	0.1423
	π	-0.9879	0.7575	6.2145	-3.8546	7.2024	0.0293	0.1406
	3π/2	-0.9949	0.7507	6.2373	-3.8632	7.2322	0.03	0.1378
	2π	-1.0047	0.7413	6.2674	-3.8754	7.2721	0.031	0.1339
0.14	0	-1.1373	0.7629	3.2673	-3.9671	4.4046	0.0234	0.1526
	π/2	-1.1383	0.7619	3.2625	-3.9684	4.4008	0.0236	0.1521
	π	-1.1415	0.7589	3.248	-3.972	4.3895	0.0241	0.1507
	3π/2	-1.1467	0.7539	3.2243	-3.9782	4.371	0.0251	0.1484
	2π	-1.154	0.7471	3.1921	-3.9869	4.3461	0.0265	0.1452
0.16	0	-1.2786	0.7689	2.8893	-4.0899	4.1679	0.0399	0.1573
	π/2	-1.2794	0.7681	2.8868	-4.0908	4.1662	0.0401	0.1569
	π	-1.2816	0.7659	2.8796	-4.0934	4.1612	0.0407	0.1558
	3π/2	-1.2854	0.7623	2.8676	-4.0977	4.153	0.0416	0.1539
	2π	-1.2907	0.7573	2.8511	-4.1038	4.1418	0.043	0.1514
0.18	0	-1.4072	0.7789	2.6636	-4.2171	4.0708	0.0599	0.1559
	π/2	-1.4078	0.7784	2.6623	-4.2177	4.0701	0.0601	0.1556
	π	-1.4093	0.7768	2.6583	-4.2195	4.0676	0.0606	0.1548
	3π/2	-1.4119	0.7742	2.6517	-4.2225	4.0636	0.0614	0.1534
	2π	-1.4156	0.7705	2.6425	-4.2267	4.0581	0.0626	0.1514
0.2	0	-1.5244	0.7913	2.5165	-4.3497	4.0409	0.082	0.1481
	π/2	-1.5248	0.7909	2.5157	-4.3501	4.0405	0.0822	0.1479
	π	-1.5258	0.7897	2.5135	-4.3513	4.0393	0.0826	0.1472
	3π/2	-1.5276	0.7878	2.5097	-4.3533	4.0373	0.0833	0.1462
	2π	-1.53	0.7852	2.5045	-4.3561	4.0345	0.0842	0.1448

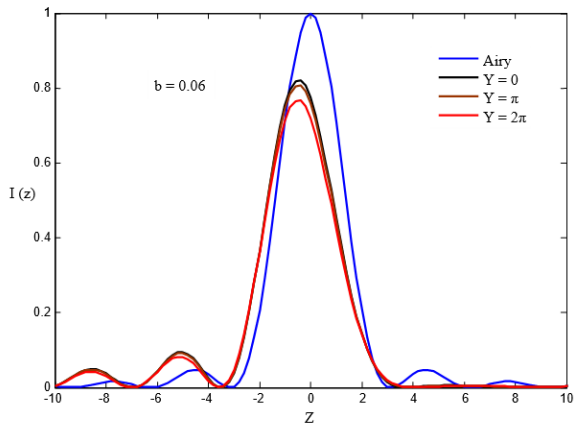

Fig. 2 Intensity profile of PSF for different defocused image planes with optimized anti-phase apodization of edge strips (b = 0.06).

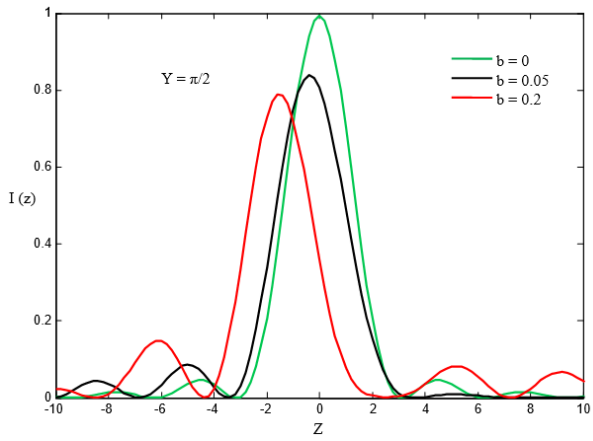

Fig. 3 Intensity Profile of PSF for various values of edge strip width b when the image plane is at Y = π/2.

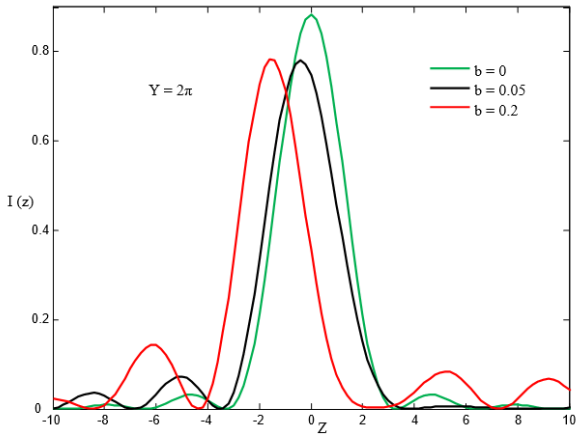

Fig. 4 Intensity Profile of PSF for various values of edge strip width b when the image plane is at Y = 2π.

Table 1 shows the maxima and minima and respective intensities in the asymmetric PSF for different out-of-focus planes. These parameters are computed for various values of defocusing controlling parameter (Y) varying from 0 to 2π in steps of π/2 for different amount of asymmetric apodization. b is the edge strip width of the slit aperture which controls the degree of asymmetric apodization.

The defocused optical imaging systems with asymmetric apodization considered in this study are assumed to be shift variant and diffraction limited. The relation between the analytical design of complex pupil function and the asymmetric PSF is established mathematically. For b = 0, there is a steady decrease in the central peak intensity as Y increases from 0 to 2π i.e. width of the central peak increases from 3.1416 to 3.3084 and there is also a decrease in the first secondary maximum intensity indicating a clear suppression of optical side-lobes. This aspect is an interesting observation one from the point of resolution ability of the defocused optical imaging systems. For b = 0.02, the central peak shifts for all values of Y. It is observed that the central peak is moving away from the diffraction center as amount of defocusing in the image plane increases. This can be seen in more detail from the listed values in Table. I and also shown in Fig.5. Similar trend is noticed for all values of edge strip width b there by rendering the resolving nature of the defocused optical systems of the very faint object in the close proximity of bright object.

The position of first minimum (FMP) with respect to z = 0 (diffraction center) has been evaluated for different values of edge strip width (b) and listed in Table. I, for in-focus and out-of-focus image planes. From these values it is found that first minimum initially moving away from and then approaching to the diffraction center with the increase in edge strip width b for all the values of defocusing parameter Y. For an instance, as defocusing in the image plane increases from 0 to 2π, the first side-lobe on good side is moving from 2.5165 to 2.5045 when the edge strip width is b = 0.2. The same trend has noticed in Fig.7. So it concludes that the central spot size is sinking i.e. narrowing the central peak on good side of the diffraction pattern in addition to extension of the first minima on good side with zero intensity creating a dark region which renders the improvement in the resolution of composite image of two line objects under defocusing effect. This is one of the merits of our current study. This trend is not found for other values of b like 0.12, 0.14 and 0.16 for which the defocusing effect degrades the resolution of the PSF. So this effect became optimum for only b = 0.2. The absolute values of first minima positions (FMP) under the same conditions but with respect to central maxima position (CMP) have been studied and listed as FMP w.r.to CMP in Table. I. Based on these values it can be said that the resolution of defocused optical system is turning down. It can be seen in more detail from Fig.8. In the presence of defocusing, as b increases from 0 to 0.06 there is a significant improvement in overall resolution of the defocused PSF. On further increase of b value it is found that sidelobe intensity increases.

First optical side-lobe intensity (FSI) on good side of the diffraction pattern have been studied for different values of edge strip width b. These values have been obtained for various values of Y and the same presented in Fig.6. For b = 0.02, there is steady decrease in the first side-lobe intensity on good side as defocusing in the image plane is increasing from 0 to 2π and also found that the side-lobe intensity is suppressing from 0.0056 to 0.0042 for b = 0.06. This indicates that for optimized anti-phase apodization of edge strips (b = 0.06), for a maximum defocused image plane (Y = 2π) we obtained maximum suppression for side-lobes on good side of the diffraction pattern. This is nearly 90% lower than the value obtained in unapodized case. On further increase in edge strip width b, the first side-lobe intensity increases with defocusing parameter Y. This effect can be seen clearly in Fig.2 in which a solid blue line curve represents Airy PSF for easy comparison with the PSF obtained from different out-of-focus planes. 3-D intensity profile of Airy PSF is depicted in Fig.9. Fig.3 shows that for partially defocused image plane (Y = π/2), we obtained improved side-lobe suppression and occurs at edge strip width b=0.05. For a maximum defocused plane (Y = 2π), the maximum suppression of side-lobe is occurs at same edge strip width b=0.05. It is clearly depicts in the Fig.4. These curves are also demonstrate that, for Y = π/2 and b = 0.2 there is small dark zone has created on good side in the vicinity of the central maxima and it spreads out little for maximum defocused image plane (Y = 2π). This small dark zone is particularly important to detect the direct image of faint object which is in the close proximity of very bright object. For all values of edge strip width b, as defocusing in the image plane increases from 0 to 2π the first minimum position on bad side is moving away from diffraction center (z=0) and mean while the intensity of first side-lobe on bad side is increasing progressively. This can be seen in more detail from the listed values in Table. I. This study is also concluded

that the pattern on good side of the PSF is obtained at the cost of the pattern on bad side of the PSF.

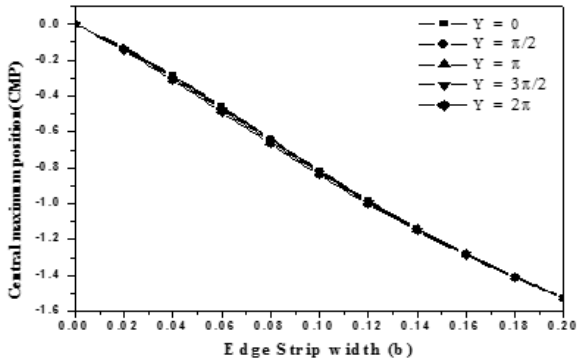

Fig. 5 Shifting of central maximum with an edge strip width b for different defocused image planes.

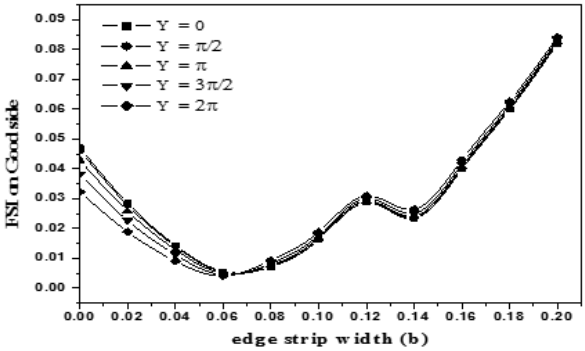

Fig. 6 Curves showing variation of first side lobe intensity on good side with an edge strip width b for different defocused image planes.

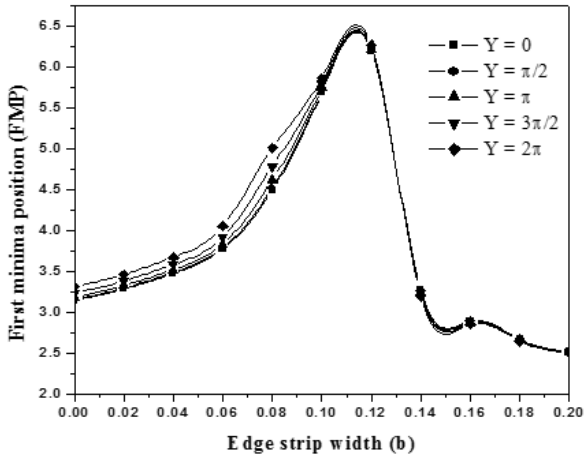

Fig. 7 First minimum position with respect to z=0 as a function of b for different values of defocusing controlling parameter Y.

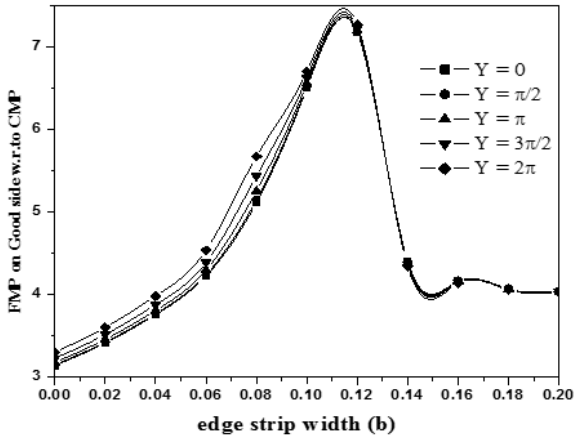

Fig. 8 First minimum position with respect to central maxima position as a function of b for different defocused image planes.

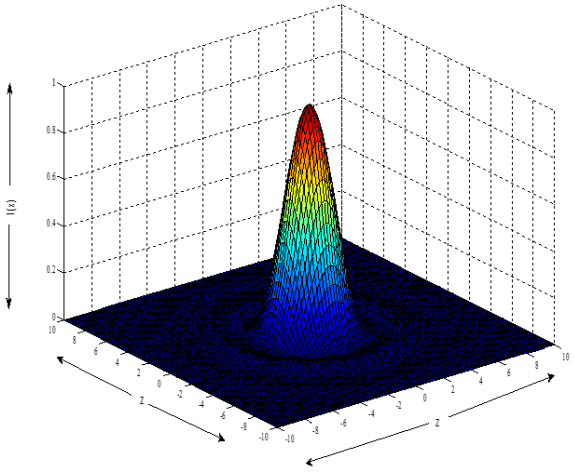

Fig. 9 3-D Representation: Airy PSF of Optical imaging system with One-dimensional pupil filter.

4 Conclusions

From present studies we can conclude that in the presence of defocusing there is a significant improvement in the resolution of asymmetrically apodized optical systems in the case of one-dimensional complex pupil functions. The maximum suppression of first side-lobe on good side of the PSF is found at b = 0.06 for a maximum defocused image plane. For Y = 2π and b = 0.2, the central peak becomes narrower on good side and there is a small dark region is produced in the vicinity of the central peak. On the whole it can be emphasized that defocusing is found to be more effective in enhancing the resolution of two line objects. For Airy PSF, side-lobe suppression on good side is found to decrease with an increase of defocusing effect (Y) in the image plane and it is further improved by the degree of asymmetric apodization (b) of slit aperture. These characteristics would make the system more effective in resolving the composite image of two line objects which are widely varying in their intensities.